Published in final edited form as:
Lab Chip. 2010 April 7; 10(7): 918–920. doi:10.1039/b919614e.

Controlled Reagent Transport in Disposable 2D Paper Networks

Elain Fu[*], **Barry Lutz**, **Peter Kauffman**, and **Paul Yager**

Abstract

Recent reports have demonstrated the multi-analyte detection capability of paper networks with multiple outlets per inlet. In this report, we focus on the capabilities of 2D paper networks with multiple inlets per outlet and demonstrate the controlled transport of reagents within paper devices. Specifically, we demonstrate methods of controlling fluid transport using the geometry of the network and dissovable barriers. Finally, we discuss the implications for higher sensitivity detection using this type of 2D paper network.

Introduction

Paper-based lateral flow immunoassays have been commercialized for use in applications ranging from home pregnancy tests to point of-care detection of infectious disease antigens and the antibodies produced against them. These strips can be inexpensive, are well suited to storage of reagents in dry form, output a signal that is readable by eye, and because they use capillarity to move fluids, require no supporting pumps or pressure sources. However, current tests lack the sensitivity required to have clinical utility for a number of targets and usually only measure a single analyte per strip.[1] The utility of lateral flow assays would be significantly increased if they were more sensitive, as evidenced by efforts to improve lateral flow assay sensitivity using a variety of particle labels (*e.g.*, quantum dots, up-converting phosphors, and paramagnetic particles).[2] In many of these cases, improved sensitivity requires increased complexity and instrumentation[3] (*e.g.*, a specialized light source, optics, and fluorescence detector), and results in a significant increase in the cost per test such that the test is no longer appropriate for many low-resource settings. In order to have a high impact in these settings, a test should maintain the ease-of-use and low cost per test of current conventional lateral flow tests, while extending the capabilities of those current tests.

Recent work has demonstrated the ability of complex paper networks to perform multiple tests on a single sample in parallel.[4–7] In this report, we investigate the processing capabilities provided by *convergence* of reagents from multiple inlets to a common detection region. This capability of 2D paper networks can be used to autonomously drive multi-step sequences. We demonstrate several methods of controlling the transport of fluid in 2D paper networks and discuss the potential for extended processing capabilities (as compared to current lateral flow tests) that could result in significant improvements in sensitivity.

Experimental

The paper devices were composed of backed nitrocellulose (Millipore, Billerica, MA) cut by a CO_2 laser(Universal Laser Systems, Scottsdale, AZ). The smallest lateral dimension of the devices was 3 mm except in the case of the trehalose Y-shape devices in which the smallest

Box 355061, Department of Bioengineering, University of Washington, Seattle, WA. Fax: 1-206-616-3928; Tel: 1-206-685-9891; efu@u.washington.edu.

lateral dimension was 1.5 mm. Reagents were introduced to an absorbent pad (Millipore, Billerica, MA) in contact with an inlet (~50 and 80 μl from a syringe for the demonstrations in Figures 2 and 3, respectively). The same absorbent material was used for the wicking pad in the 3-inlet device experiments. Double-sided tape (3M, St. Paul, MN) on a glass substrate (Thermo Fisher Scientific, Waltham, MA) was used to support the device. For the trehalose experiments, an absorbent pad containing trehalose (Sigma-Aldrich, St. Louis, MO) in water (~40% by weight) was used to create a stripe of trehalose across the nitrocellulose strip, and the stripe allowed to dry overnight. For the 3-inlet device experiments of Figure 4, a different volume of reagent solution was introduced to each of the absorbent pads at the 3 inlets (~17, 25, and 35 μl, using a multi-channel pipette, for the inlets from right to left, respectively). For the 3-inlet device experiment of Figure 4b, a dried flake of the pH indicator Bromothymol blue (Aldrich, Milwaukee, WI) was placed in the common segment of the device to detect pH after the introduction of buffer solutions (EMD Chemicals, San Diego, CA) to the inlets (pH 10, 4, and 10 for the inlets from right to left, respectively). Food coloring was used in the other demonstration experiments. After application of fluid(s) to the abosorbent pad(s), devices were kept in a covered petri dish containing a water source to minimize evaporation. Images were adjusted for improved contrast and brightness levels.

Results

In 2D paper networks, as in lateral flow devices, capillarity of the paper and a downstream wicking pad produce fluid flow through the paper pores. These devices support plug flow rather than the Hagen-Poiseuille flow characteristic of many microfluidic devices (pressure-driven flow at low Re). This offers the advantage of reducing Taylor-Aris dispersion and allowing delivery of reagents with reduced intermixing. The movements of multiple species within the system are determined by a few factors, the most important of which are the dimensions of individual paper segments and their configuration within the network. Creating multi-step processes in 2D paper networks requires control of fluid transport in the networks.

Figure 1 shows three simple methods for controlling the flow in paper networks of uniform thickness. First, it is well known that in a segment of constant width, movement of the fluid front advancing into a dry membrane depends on the resistance that the wet paper behind it presents to flow of the lengthening column of fluid. This viscous resistance increases with length, so the further the front moves, the slower it moves, according to the Washburn equation, $L^2 = \gamma Dt / 4\mu$, where L is the distance moved by the fluid front, t is time, D is the average pore diameter, γ is the effective surface tension (which includes the effect of any contact angle dependence), and μ is viscosity.[8] Second, a change in the width of a segment within a network can be used to vary the transport time of the fluid front within that segment of the network. Third, dissolvable barriers can delay fluid movement in segments of the network. The composition of the device materials, pore size, and surface chemistry also affect the flow rate, but were not investigated here.

Figure 2 shows experimental demonstrations of two of the methods of controlling fluid transport proposed in Figure 1. Figure 2a shows a sequence of images of fluid transport for 2 paper configurations; (1) a constant width paper strip, and (2) a wider paper strip that is fed by an inlet of the same width as in (1). The image sequence of Figure 2a shows that the fluid front moves a greater distance downstream in the narrower width strip as compared to the wider width strip for a given time interval. Figure 2b shows plots of the distance travelled by the fluid front vs. time for each of the strips. The inset plot shows that both are consistent with Washburn-like flow, with a smaller slope for the strip of greater width.

Figure 3 shows a simple demonstration of the use of a dissolvable barrier to produce a delay in the transport of reagent to its destination. In this case, the dissolvable barrier was created by application of a solution of trehalose, and subsequent drying of that solution. Fluid wicks up to the barrier and is slowed during dissolution of the soluble material. After barrier dissolution, the fluid moves freely into the region beyond. Figure 3a shows a delay in fluid transport in the right fork of the device, due to the initial presence of a trehalose barrier in the right fork. The initial extent of the barrier and the rate of barrier dissolution determine the delay in transport of the reagent.‡‡ Figure 3b shows that a barrier of greater extent results in a longer delay for the fluid.

Sequential reagent delivery to a "detection region" is experimentally demonstrated in Figure 4 using a paper network with 3 staggered inlets to the common (horizonal) segment of the device. Increasing volumes of reagent were introduced into the inlets (via the absorbent pads) from right to left, respectively. The fluid with the shortest path, from the rightmost inlet, reaches the detection region first and runs out first, while the fluid with the longest path, from the leftmost inlet, takes the longest time to reach the detection region and runs out last. Figure 4a shows the delivery of 3 colored fluids, orange, red, and yellow, while Figure 4b shows a demonstration of pH change from pH 10 to 4 to 10 as different buffers from the 3 inlets are sequentially delivered to the pH indicator flake located near the wicking pad. The timing for delivery of multiple fluids, i.e. arrival times and duration of flows, can be varied by changing the path length for fluid travel from each inlet and the volume of fluid applied to each inlet. Choice of these parameters, along with the fluid capacity of the materials used, will also determine the amount of time the reagent flows will overlap. This can be tailored as needed for the requirements of the specific application.

Discussion

The use of two intersecting paths to sequentially deliver analyte and labels to a detection region has been reported to result in a 10–50× improvement in sensitivity[9]. In this investigation, we have demonstrated several simple methods of controlling the transport of fluid in 2D paper networks that can be used to create sophisticated multi-step processes that are not possible in current lateral flow tests (including the above). Creating a multi-step process in 2D paper networks only requires engineering the fluid flow rate and the length of travel in the network. The methods shown here enable more sophisticated processes such as chemical amplification, which require multiple reagent delivery and wash steps, and have long been used to increase the sensitivity of laboratory-based bioassays. The expected result is higher-sensitivity detection with the ease-of-use and cost comparable to conventional (non-instrumented) lateral flow tests. An investigation of the resulting improvement in sensitivity in a simple system is ongoing in our laboratory.

Acknowledgments

We acknowledge Paolo Spicar-Mihalic for use of his nitrocellulose cutting method, and the support of NIH Grant No.RC1EB010593.

References

1. O'Farrell, B. Lateral Flow Immunoassay. Wong, R.; Tse, H., editors. New York: Humana Press; 2009. p. 1-33.

‡‡Note that since the surface tension is a critical parameter in the Washburn equation, if the solute changes the surface tension of the fluid, this can also cause flow after the barrier to be different than before it.

2. Chun, P. Lateral Flow Immunoassay. Wong, R.; Tse, H., editors. New York: Humana Press; 2009. p. 75-94.
3. Faulstich, K., et al. Lateral Flow Immunoassay. Wong, R.; Tse, H., editors. New York: Humana Press; 2009. p. 75-94.
4. Fentonet E, et al. Applied Materials and Interfaces. 2009; 1:124–129.
5. Martinezet AW, et al. Angewandte Chemie-International Edition. 2007; 46:1318–1320.
6. Martinez AW, et al. Proceedings of the National Academy of Sciences of the United States of America. 2008; 105:19606–19611. [PubMed: 19064929]
7. Martinez AW, et al. Lab on a Chip. 2008; 8:2146–2150. [PubMed: 19023478]
8. Washburn EW. Physical Review. 1921; 17:273–283.
9. Chembio Diagnostic Systems, Inc. 2009 April 14. <http://www.chembio.com/newtechnologies.html>.

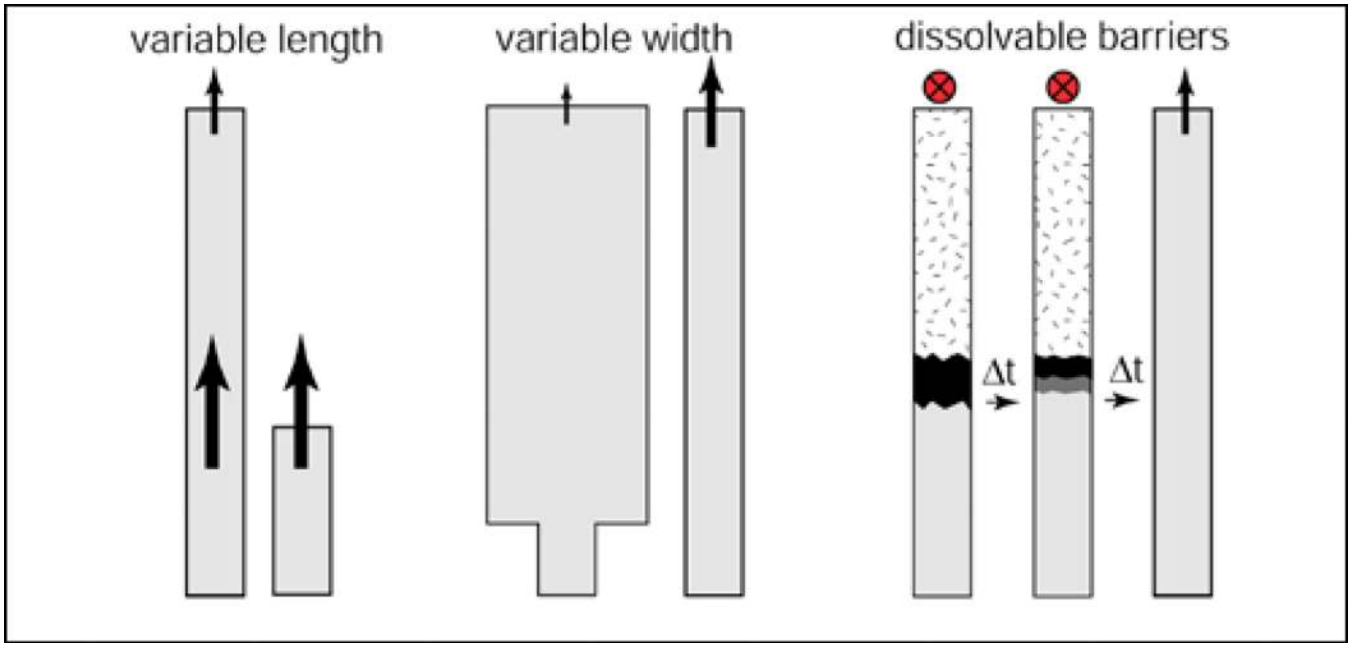

Figure 1.
The transport time through a paper segment can be controlled via length, a change in width, or the use of a dissolvable barrier (in contrast to the permanent hydrophobic barriers used to create channel walls of Martinez et al.[7]).

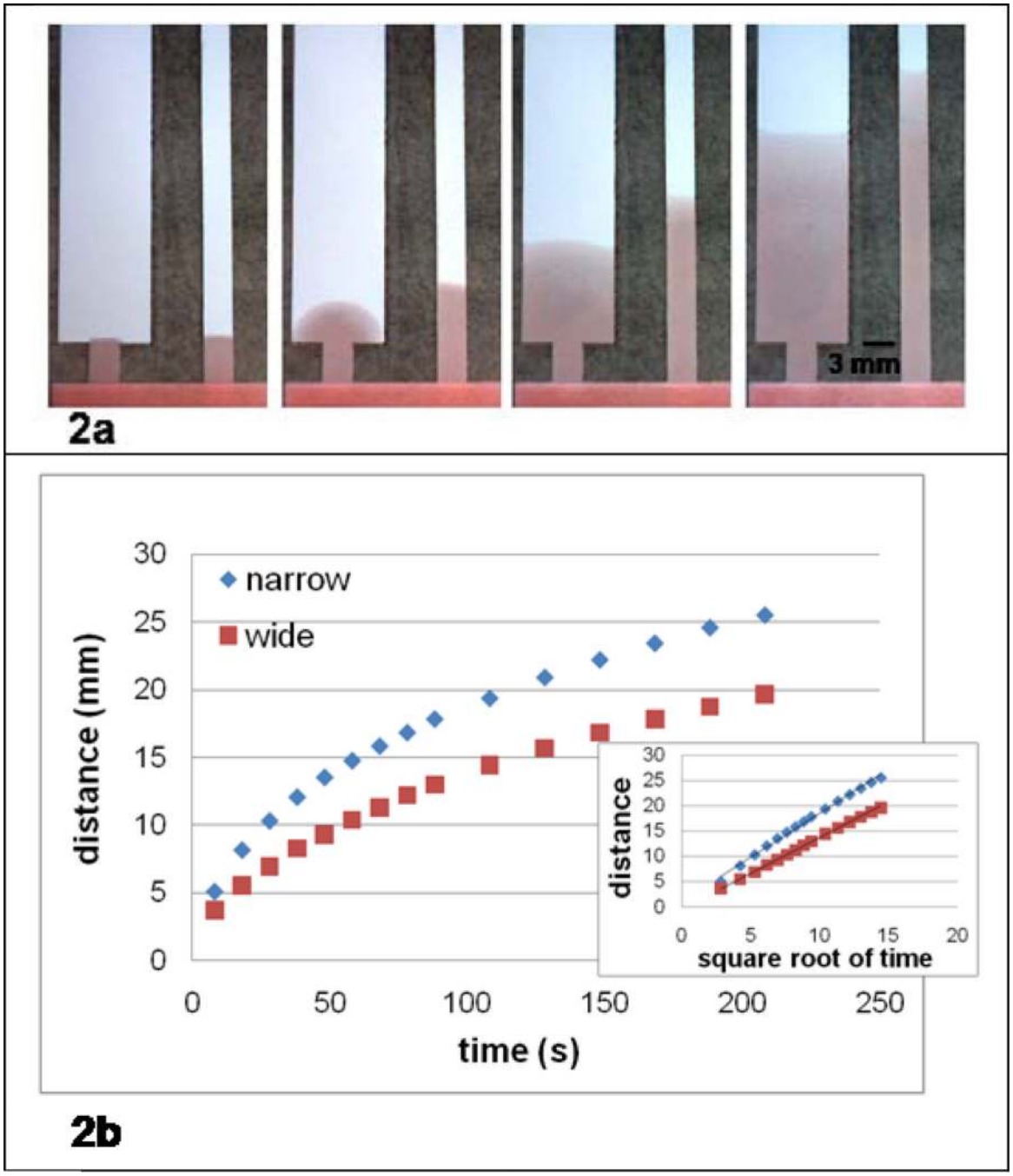

Figure 2.

Demonstration of the dependence of flow rate on the length and width of the paper strip. (a) Image sequence of flow in strips of different width (fed by the same width inlet) shows faster transport in the strip of smaller width. Images were taken at ~2, 10, 50, and 210 s after introduction of fluid to the inlet. (b) Plot of time vs. downstream distance of the fluid front for each of the strips. Within a strip, the times required for the fluid front to move the same distance increase with increasing distances downstream. The inset shows a linear relationship, consistent with Washburn-like flow. The zero time in the plots corresponds to the leftmost image of (a), i.e. when the front has reached the end of the narrow inlet of the wider strip.

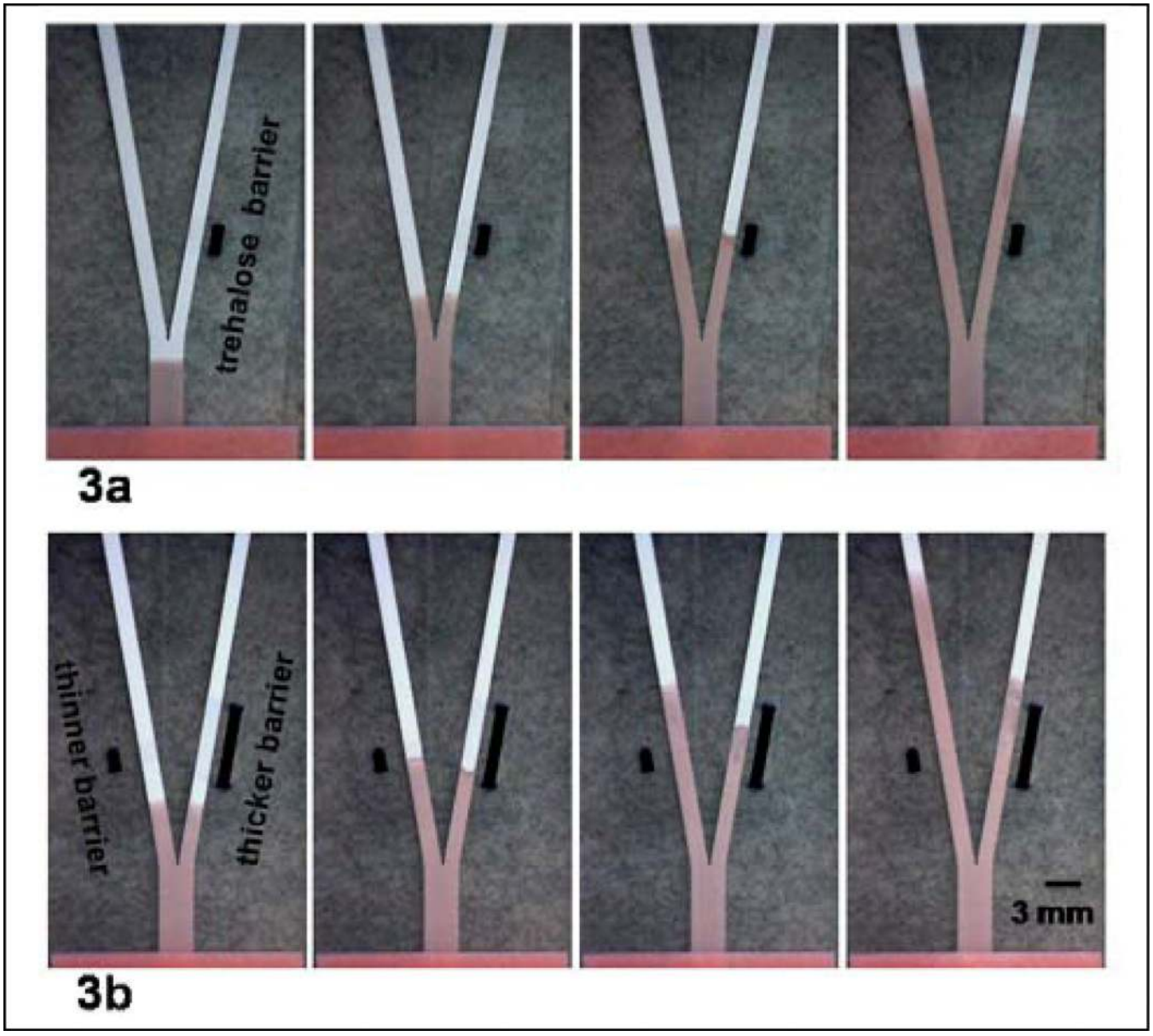

Figure 3.

A dissolvable barrier can be used to create a delay in the transport time of a fluid. (a) A dissolvable trehalose barrier was created in the right fork of the device and produces a delay in the transport of fluid in the right fork. Images were taken at ~4, 19, 49, and 159 s after introduction of fluid to the inlet. (b) Trehalose stripes of different thicknesses were applied across the left and right forks of the Y-shape device. The stripe of greater thickness in the right fork of the Y-shape device produces a longer delay in the transport of fluid as compared to the delay produced in the left fork by the trehalose stripe of smaller thickness. Images were taken at ~18, 33, 73, and 158 s after introduction of fluid to the inlet. The thick black bars approximately mark the initial extents of the trehalose barrier.

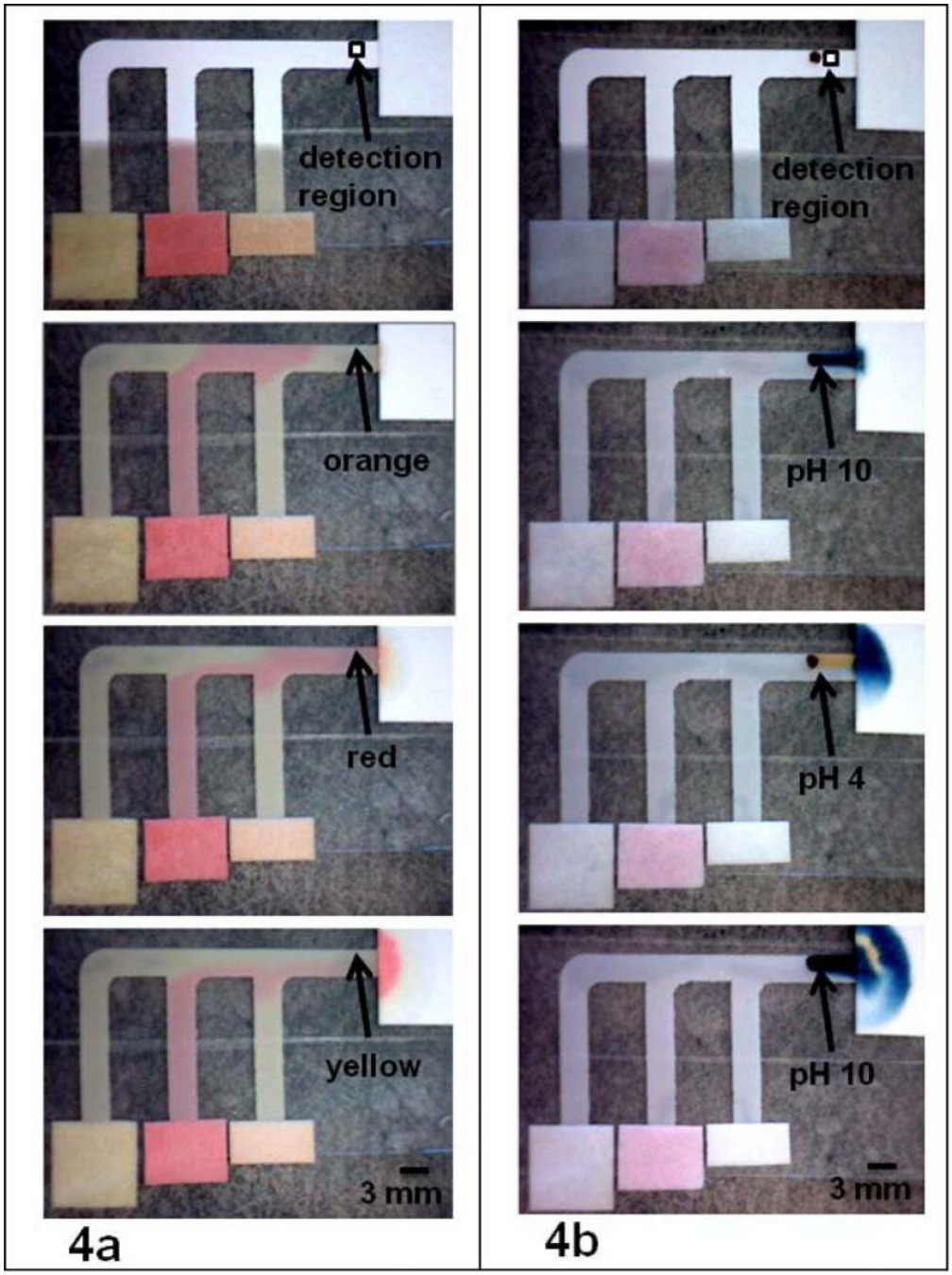

Figure 4.

Demonstration of programmed fluid delivery using a simple 2D paper network. The arrival time of multiple reagents at the "detection region" of the paper strip is staggered by placing 3 inlets along the common segment of the device. The geometry of the inlets results in the sequential arrival of fluid from each of the three inlets; (a) orange, red, and yellow colored fluid‡, and (b) buffers of pH 10, 4 and 10 that produce a change in the color of the pH indicator from blue to yellow to blue. Images are representative of the flow patterns at ~10 s, 5 min, 15 min, and 35 min in (a) and at ~10 s, 5 min, 11 min, and 20 min in (b).

‡Note that in the demonstration of Figure 4a, there is some overlap in the flow of reagents in the common segment of the device. If minimal overlap of reagents to a detection region is required for a given application, the detection region can either be limited to a region in the upper portion of the common segment (as noted in the top panels of Figure 4), or the extent of overlap of fluid delivery can be modified as described in the main text.